Water Resources Research

RESEARCH ARTICLE
10.1029/2019WR025313

Key Points:
- Precipitation-runoff relationships are influenced by variation in annual and seasonal storage
- Wet and dry multiyear precipitation patterns did not influence event-based rainfall-runoff responses
- Thick glacial till and permeable bedrock have large storage capacities

Supporting Information:
- Supporting Information S1
- Figure S1
- Figure S2

Correspondence to:
S. A. Spencer,
saspence@ualberta.ca

Citation:
Spencer, S. A., Silins, U., & Anderson, A. E. (2019). Precipitation-Runoff and storage dynamics in watersheds underlain by till and permeable bedrock in Alberta's Rocky Mountains. *Water Resources Research*, *55*, 10,690–10,706. https://doi.org/10.1029/2019WR025313

Received 5 APR 2019
Accepted 25 NOV 2019
Accepted article online 11 DEC 2019
Published online 12 DEC 2019

Precipitation-Runoff and Storage Dynamics in Watersheds Underlain by Till and Permeable Bedrock in Alberta's Rocky Mountains

S. A. Spencer[1], U. Silins[1], and A. E. Anderson[1,2]

[1]Department of Renewable Resources, University of Alberta, Edmonton, Alberta, Canada, [2]Water Program, fRI Research, Hinton, Alberta, Canada

Abstract The complex mechanisms driving runoff dynamics in mountainous watersheds with thick glacial till and fractured bedrock are not well understood. We examined long- and short-term precipitation-runoff relationships and quantified subsurface storage in watersheds on the eastern slopes of Canada's Rocky Mountains to develop a conceptual understanding of runoff generation processes in this region. Fractured permeable bedrock (bedrock storage) and glacial till deposits (soil and till storage) collectively result in large dynamic storage (hydrologically active storage). The transition from multiyear dry to multiyear wet patterns increased specific discharge due to less bedrock storage opportunity but did not influence event-scale rainfall-runoff responses. Rather, event-scale rainfall-runoff responses were governed by snowmelt and soil and till storage capacity. While winter snowfall was an important predictor of annual runoff ratios, storage at the end of the previous fall also influenced runoff ratios. These complex subsurface dynamics and large storage capacities are important for understanding how mountainous watersheds with glacial till deposits may respond to disturbance or climate change.

1. Introduction

Runoff generation studies have often been conducted in rainfall-dominated mountainous watersheds with topographically driven runoff, local groundwater flow pathways, shallow soils, and relatively well defined impermeable bedrock boundaries (Hewlett & Hibbert, 1967; McGuire et al., 2005; Mosley, 1979; Uchida et al., 2003). These characteristics lead to a low subsurface storage capacity (Buttle et al., 2004) and short mean transit times (Pfister et al., 2017). Conversely, in mountainous regions with thick surficial deposits, thick soils, or permeable fractured bedrock, subsurface storage capacity can be large (Gabrielli et al., 2012; Hale et al., 2016) and mean transit times can be long (Hale & McDonnell, 2016). These differences in watershed storage may also influence how a watershed responds to climate change or forest disturbance (e.g., wildfire and insect outbreak). Increases in surface air temperatures due to climate change may increase the proportion of rain to snow, advance the timing of snowmelt, and reduce total snowpack water inputs in high elevation mountainous regions (Rasouli et al., 2019). Additionally, forest disturbance can also increase precipitation inputs to the forest floor (Boon, 2012; Williams et al., 2019). These changes may directly affect the timing and quantity of runoff in responsive watersheds with low subsurface storage capacity (Stednick, 1996; Winkler et al., 2017), whereas watersheds with greater storage capacity may buffer the change in precipitation inputs thereby muting the impacts associated with forest disturbance and climate change (Harder et al., 2015). However, the mechanisms controlling this potential damping of disturbance effects on streamflow are poorly understood.

Bedrock permeability and its effects on storage and release of water have been the focus of recent multiwatershed comparison studies. Uchida et al. (2006) compared two physically similar steep watersheds with shallow soils in humid and wet climates but with different bedrock permeability and water retention characteristics (Maimai, New Zealand, and Fudoji, Japan). Higher bedrock permeability and soil drainable porosity in Fudoji resulted in longer mean residence times and larger potential storage, which in turn lead to more stable baseflows. Hale and McDonnell (2016) compared transit times for watersheds with weathered fractured sedimentary bedrock in the Oregon Coast Range and less permeable volcanic bedrock in the Western Cascades Range and found that shallow lateral flow and shorter mean transit times were more prevalent in watersheds with less permeable bedrock. Similarly, Pfister et al. (2017) reported longer mean transit times with greater bedrock permeability for 16 watersheds in Luxembourg. In watersheds with less permeable bedrock, storage was more likely to be filled quickly resulting in a clearer precipitation-runoff threshold behavior during wetter periods. Conversely, dampened peak flows and higher winter baseflows were observed in watersheds with highly permeable bedrock (Pfister et al., 2017).

The presence of glacial till deposits or deep soils has also been shown to add complexity to subsurface flow pathways, storage, and precipitation-runoff dynamics (Detty & McGuire, 2010a; Nippgen et al., 2016) and can lead to very different hydrograph recession characteristics between neighboring watersheds (Shanley et al., 2015). Climatic variation and antecedent conditions such as interannual variation in precipitation amount or seasonal precipitation patterns were critical in explaining groundwater table responses, landscape connectivity, and streamflow responses to precipitation in many studies (Detty & McGuire, 2010a, 2010b; Devito et al., 2012; Gannon et al., 2014; Nippgen et al., 2016; Tomasella et al., 2008). For instance, Devito et al. (2012) showed that antecedent precipitation from the previous years and seasons regulated watershed storage and precipitation-runoff patterns in subsequent years. Detty and McGuire (2010a) described runoff thresholds associated with groundwater levels and the sum of antecedent soil moisture plus total precipitation.

Although runoff generation has been described for regions with fractured permeable bedrock or thick soils and till individually, few studies have been conducted in mountainous regions with both (e.g., Burns et al., 1998; Dahlke et al., 2012; Shaman et al., 2004). Burns et al. (1998) showed that groundwater from both glacial till and permeable fractured bedrock sustained baseflow and added complexity to runoff generation dynamics. Antecedent conditions regulated stormflows in a watershed where deep flow pathways below fragipan layers generated most of the stormflow during dry antecedent conditions (Dahlke et al., 2012). Conversely, near surface flow was an important contributor during wet antecedent conditions because the clay expanded and cracks in fragipan closed (Dahlke et al., 2012).

In Canada's southern Rocky Mountains, fractured sedimentary bedrock is common and does not form an impermeable boundary to impede the percolation of water. Furthermore, the region is overlain by thick glacial till composed of highly heterogeneous deposits (fine through very coarse sediments, cobbles, clay lenses, etc.) adding complexity to subsurface storage and flow pathways that are not evident from surface topography alone (Langston et al., 2011). Glacial deposits have been shown to regulate groundwater storage and contributions to streamflow throughout the year in the Opabin moraine (Langston et al., 2011). Other studies have shown that storage in talus slopes is a key contributor to autumn low flows (Hood & Hayashi, 2015; McClymont et al., 2010). This region is snow dominated, and peak flow is often determined by the snow water equivalent in the alpine zones because it contributes the most water to the stream (Harder et al., 2015). Snowmelt can recharge groundwater (Smith & Redding, 2012) or overwhelm percolation rates and result in perched water tables and lateral flow to the stream (Kuras et al., 2008; Smith et al., 2014). Due to this enhanced recharge, summer low flows in alpine watersheds can depend on snow accumulation in winter (Jenicek et al., 2016). While these studies have elucidated some runoff generation processes in mountainous watersheds with glacial till, conceptual understanding of runoff generation and storage dynamics in watersheds with thick uncompacted tills over permeable bedrock remains incomplete.

Star Creek is a long-term instrumented watershed in the eastern slopes of the Rocky Mountains (Figure 1) and a part of the Southern Rockies Watershed Project (SRWP). The SRWP investigated, among other objectives, the hydrological implications of three harvest treatments in Star Creek's subwatersheds. Runoff is generally thought to be topographically driven, but thick, heterogeneous surficial deposits from the Wisconsin glaciation may create complex subsurface flow that may not follow the surface or bedrock topography. In order to interpret or predicted differences in watershed responses to harvest treatments, a conceptual understanding of runoff generation and the effects of subsurface characteristics on precipitation-runoff relationships in the eastern slopes is needed. Thus, the main objective of this study was to characterize precipitation-runoff relationships in two adjacent Rocky Mountain watersheds with thick surficial glacial deposits overlaying highly fractured permeable bedrock. The research approach included characterizing (1) both long-term (annual) and short-term (seasonal and event-based) variation in precipitation-runoff relationships and (2) spatial variation in precipitation-runoff relationships and storage for two adjacent subwatersheds.

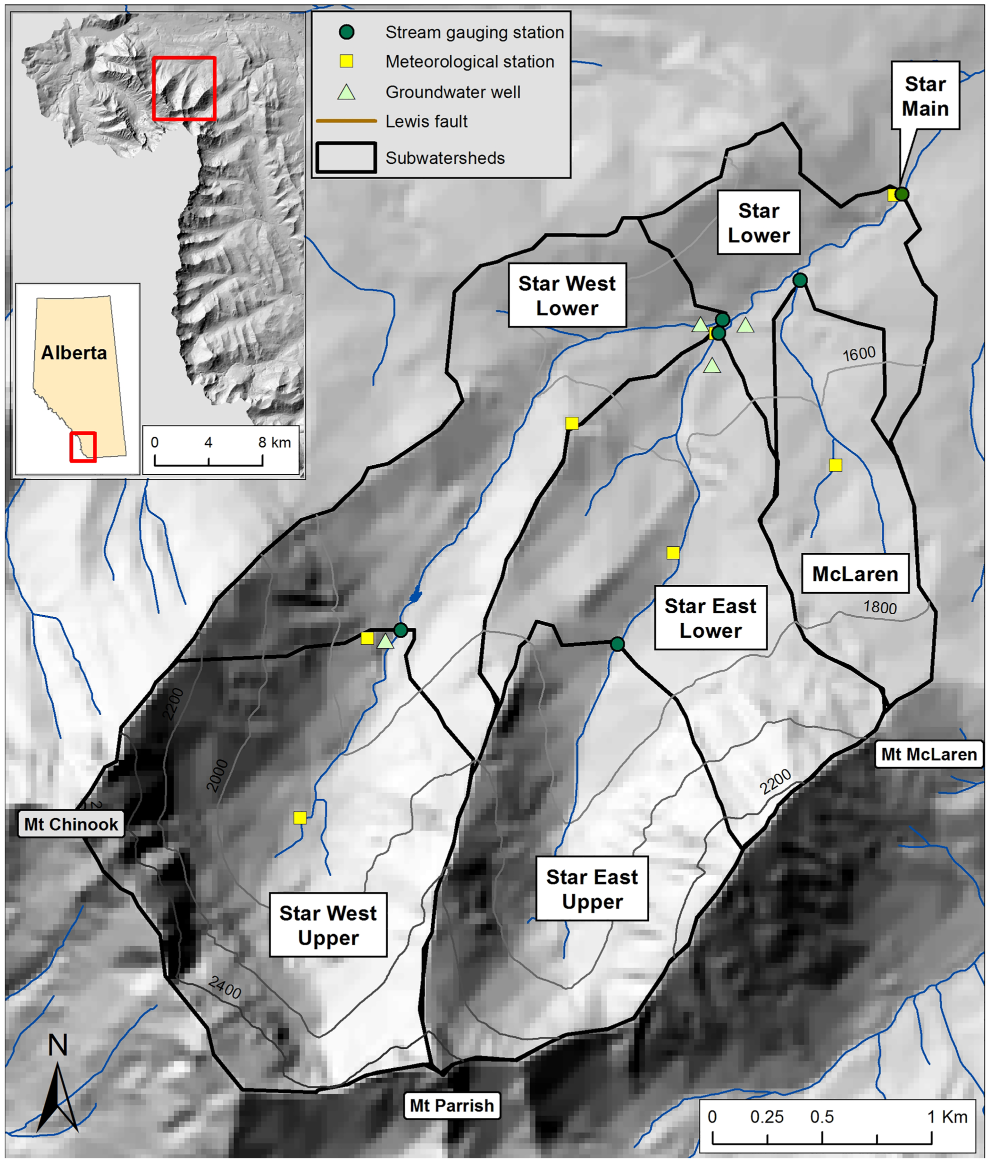

Figure 1. Map of Star Creek watershed in southwest Alberta, Canada.

2. Study Site

Star Creek (10.4 km^2) is a snowmelt-dominated watershed with peak streamflow typically occurring in late May. Average precipitation is 990 mm yr^{-1} in the subalpine area (1,732 m above sea level, a.s.l.) and 720 mm yr^{-1} in the lower part of the watershed at Star Main (SM; 1,482 m a.s.l.). Precipitation falls as snow from October to April or May (50–60% of annual precipitation); summer convective storms and autumn rains dominate precipitation in the warmer months (June to September). Mean monthly temperatures range from 15 °C in July to −6.5 °C in December. The stream is comprised of two main tributaries, Star East (SE) and Star West (SW), and a smaller ephemeral stream (Star McLaren). This study focuses on SE (3.9 km^2; 1,540–2,516 m a.s.l.) and SW (4.6 km^2; 1,537–2,628 m a.s.l.) subwatersheds, which are separated into upper and lower sections (Figure 1).

The forest is dominated by lodgepole pine (*Pinus contorta*) and subalpine fir (*Abies lasiocarpa*), with small portions of Engelmann spruce (*Picea engelmannii*), white spruce (*Picea glauca*), trembling aspen (*Populus tremuloides*), and Douglas fir (Pseudotsuga menziesii *var. glauca*). In the alpine area (>1,900 m), small shrubs and grasses grow on bedrock and talus slopes (Dixon et al., 2014; Silins et al., 2009). Soils are

10.1029/2019WR025313

Eutric Brunisols (Can. Soil Classification, equivalent to Eutric Cambisols in Food and Agriculture Organization system) with clay loam texture and relatively weak horizon development, characteristic of cold, upper elevation mountain regions (Silins et al., 2009; D. Mueller, personal communication, August 9, 2019). Local variation in aspect, elevation, and soil moisture result in moderate to high variation in soil depth throughout the watershed, though clear surface horizons are difficult to distinguish from parent geologic material. The regional geology is composed of sedimentary bedrock from three geologic formations: Upper Paleozoic formation, Belly River-St. Mary Succession, and Alberta Group formation. In general, all formations are composed of shale and sandstone, with sporadic carbonaceous layers (AGS, 2004). The landscape has undergone glacial erosion and deposition as recent as the Wisconsin glaciation (Gov. AB., 2000). The surficial geology is composed primarily of colluvium, talus slopes, and slightly leached till. Glacial till is 3 m thick on average (AGS, 2004) but depths greater than 10 m have been observed. Cirque tills (<10 m depth) are present in the alpine area of Star West subwatershed (AGS, 2004). Unsorted, uncompacted supraglacial till are common throughout the watershed; some clay-rich lodgement till has also been observed.

The SW subwatershed has two natural reservoirs, a marshy wetland in the alpine area and a small pond below the Star West Upper streamflow gauge; both maintain water year-round. The pond was caused by a landslide that impounded the stream. Much of the stream above the Star West Upper gauging station flows over bedrock, whereas cobbles and pool-riffle sequences dominate the lower reaches. Permanent surface reservoirs are not present in SE subwatershed. In the upper alpine area, ephemeral stream channels are dendritic and channels are incised into colluvium rather than bedrock. Tall vertical cliffs are present in most of the upper ridges of the alpine regions in both subwatersheds, although Mt. McLaren is less vertical than Mt. Parrish and Mt. Chinook. As a result, the SE subwatershed has slightly less vertical relief (1,540–2,516 m) than the SW subwatershed (1,538–2,628 m).

3. Methods

3.1. Temporal Variation in Annual Precipitation and Streamflow

3.1.1. Precipitation

Precipitation was measured at low elevation (SM, Star Confluence, Star Bench, McLaren, and North York Main) and high elevation (Star West High, Star East High, Star Alpine, and North York High) sites from 2005 to 2014 with Jarek tipping bucket gauges (Geoscientific, Vancouver, Canada) with alter shields. Gauges were fitted with antifreeze overflow systems for measuring snow (water equivalent) during winter months. A Double Fenced Intercomparison Reference system with a weighing gauge (T-200B, Geonor Inc., Augusta, NJ, USA), located within 50 m of the North York Main precipitation site, was used to determine potential errors in precipitation estimates. Precipitation measured at these sites showed a consistent relationship and the difference between the measurements was less than 5% over 2 years of study (Cherlet et al., 2018). Precipitation measured by the Jarek tipping bucket was corrected for undercatch accordingly.

Mean area weighted annual precipitation was calculated for the watershed for each water year (WY) using the Thiessen polygon method from the distributed climate stations. While this method does not account for orographic effects, nine (seven in Star Creek and two in an adjacent watershed) distributed precipitation gauges across a range of elevations enabled a robust estimation of watershed precipitation. The standard deviation of precipitation measured for the 2005–2014 WYs across precipitation gauges was approximately 10–14% of total precipitation at a particular gauge.

The start and end dates of each WY varied and depended on the date that snow started to accumulate in the alpine area. This was based on continuous snow depth measurements (SR50 ultrasonic snow depth sensor; Campbell Scientific, Logan, UT, USA) at Star Alpine and precipitation phase (rain snow) separation after Kienzle (2008). Total annual precipitation (WY) was compared to the 10-year mean annual precipitation to identify which years were above and below the 10-year mean.

3.1.2. Streamflow

Five streamflow gauging stations were distributed throughout Star Creek. Star Main (SM), Star East Lower (SEL), and Star West Lower (SWL) stations were installed in January 2005. Star West Upper (SWU) and Star East Upper (SEU) stations were installed in October 2008. All stations have complete records from 2009 to 2014 WY. Although stream channels were relatively stable, stage-discharge relationships were developed for each of the stations for each year because channel cross sections can change over time. Stream discharge was measured with a velocity meter (SonTek/Xylem Inc., San Diego, CA, USA) 12–18 times from April to October each year based on the U.S. Geological Survey streamflow gauging protocol. Under-ice discharge was not measured during winter months. Ten-minute continuous stage data from pressure transducers (HOBO U20, Onset Computer Corp., Bourne, MA, USA) or gas bubbler systems (H350/H355 Waterlog Series, YSI Inc./Xylem Inc., Yellow Springs, Ohio, USA) were converted into discharge using the stage-discharge relationships and aggregated into average daily discharge and annual discharge. Errors in streamflow measurement are assumed at approximately ±10% based on U.S. Geological Survey and Water Survey of Canada approximations for the velocity-area method. Streamflow was measured weekly during high flows and every other week for the rest of the snow-free period to capture the large variation in streamflow.

Discharge was converted into annual unit area discharge differential ([station discharge-upstream station discharge]/subwatershed area; in mm day^{-1}) for each subwatershed as an indicator of the contribution of each subwatershed to streamflow.

3.2. Short-Term Temporal Variation in Precipitation-Runoff Relationships

3.2.1. Event-Based Rainfall-Runoff Responses

Hourly rainfall data between July and September were separated into events based on a minimum event size of 5 mm and time between events of 6 hr. Specific discharge (streamflow per unit area) was quantified at the start of the rainfall event and at the peak. The difference between specific discharge at the start of the event and at peak specific discharge was calculated for all events and referred to here as "event rise." Rainfall-runoff responses were grouped and compared across dry (2009 or 2010) and wet (2013 or 2014) years.

Four hillslope groundwater wells were installed to depth of refusal (0.8–1.5 m) in summer 2013. Wells were located 30–50 m upstream from the streamflow gauging stations at SEL, SWL, and SWU and approximately 100 m downstream from the confluence on the main stem (Figure 1). Water table depth was monitored with Odyssey capacitance loggers (Dataflow Systems Ltd., New Zealand) at 10-min intervals and a water level beeper (Heron Instruments Inc., Ont., Canada) every other week from April to October.

3.2.2. Seasonal Antecedent Conditions

Total precipitation was separated into winter precipitation (mainly snowfall), summer rainfall, and fall rainfall for each subwatershed (SE and SW) based on the Thiessen area weighted average of all precipitation gauges in and surrounding the watershed. The period covered by each category varied for each year depending on when snow started to accumulate in the alpine area (on average in late October) and when rainfall began in the spring (on average early May). Fall rainfall began 1 September each year as an estimate of when transpiration slowed significantly and groundwater levels typically started to rise. A lack of groundwater wells prior to 2013 did not allow for a dynamic classification of the start of fall rainfall. Annual runoff ratios were calculated for each WY and categorized based on total fall precipitation from the previous WY (dry fall or wet fall—below or above mean fall precipitation).

3.3. Spatial Variation in Storage

Two methods were used to estimate watershed storage to compare the similarities in results as parallel lines of evidence (Staudinger et al., 2017). These were the water balance approach and the baseflow recession approach.

3.3.1. Water Balance Approach

Watershed storage is calculated most often in rain-dominated watersheds following a pronounced dry period to identify storage thresholds that explain the delay in streamflow response (Hale et al., 2016; Sayama et al., 2011). In this study site, snowmelt dominates the hydrograph and streamflow responses start when snowmelt saturates the landscape and produces runoff. This is followed by summer conditions, where the storage drains and subsurface flow pathways likely become disconnected. Rather than identifying thresholds associated with streamflow initiation as in other studies, we were interested in identifying the drying thresholds when pathways became disconnected following spring snowmelt and the differences in these thresholds between adjacent subwatersheds.

Dynamic storage (dV), as defined in Staudinger et al. (2017), is the hydrologically active storage that considers streamflow and evapotranspiration. Note that the dynamic storage does not represent total watershed storage. dV was estimated using the water balance approach as described in Sayama et al. (2011):

$$dV = P - Q - ET \tag{1}$$

where P = precipitation, Q = discharge, and ET = evapotranspiration (see below). dV was calculated independently for each WY and represents the change in storage over the course of the WY starting at zero at the beginning of each WY. We did not include the carryover of storage from one year to the next because we did not have an estimate of storage at the start of the analysis in 2005 and the objective was to compare the annual dV range between SW and SE subwatersheds. dV as calculated by the water balance approach will be referred to as dV_{WB}.

ET was estimated for the forested and alpine (open rock) areas of each subwatershed (45% and 55% of SW, respectively, and 60% and 40% of SE, respectively). For the forested area, meteorological parameters (e.g., net radiation, temperature, relative humidity, wind direction, and wind speed) measured at SM and gap filled with data from surrounding stations were used to calculate potential evapotranspiration using the Penman-Monteith equation (Monteith, 1965). Parameters that were not measured at the meteorological station at SM were quantified based on studies conducted in Star Creek or similar regions as available. Leaf area index (2.4 $m^2\ m^{-2}$) and maximum leaf conductance (2.0 mm s^{-1}) were calculated by Karpyshin (2019) in Star Creek watershed. Maximum leaf conductance was reduced by a temperature function to represent stomatal closure due to heat stress (Stewart, 1988) and a shelter factor fixed at 0.5 for a closed forest canopy (Carlson, 1991). Area weighted average tree height for SE (13.6 m) and SW (12.8 m) were calculated from the Alberta Vegetation Inventory (AVI, 2010). Estimates of interception losses associated with the forest canopy were also included. The rainfall interception relationship as reported in Brabender (2005) for the OWL-9 site was used due to a similar leaf area index (2.6 $m^2\ m^{-2}$), forest age (115 years) and tree species (lodgepole pine) as Star Creek watershed. Snow interception and subsequent sublimation was estimated as 40% of gross snowfall (Pomeroy & Schmidt, 1993; Troendle & Meiman, 1986; Williams et al., 2019). An error of $\pm$10% in snow interception and sublimation was based on the higher range of values (40–48%) reported in Troendle and Meiman (1986) for coniferous forests in continental climates and the lower range of values (30%) in Pomeroy and Schmidt (1993) for a coniferous forest in the southern boreal forest. For the alpine area, it was assumed that summer ET would be very low; thus, the main evaporative loss was due to sublimation of snow in the winter. Alpine sublimation was estimated as 26% ($\pm$6%) of gross snowfall, which is an average of estimates for a watershed in the eastern slopes of the Rocky Mountains (MacDonald et al., 2010). The error in alpine sublimation represents the range of the values (20–32%) reported in MacDonald et al. (2010).

Although errors in dV_{WB} can arise from each water balance component, evapotranspiration is the largest source of error in dV_{WB} because it was not measured directly. Error in Penman-Monteith evapotranspiration was accounted for by adjusting the maximum leaf conductance and leaf area index within the possible values reported in Karpyshin (2019), from 1.5–2.0 mm $s^{-1}$and 2.4–4.0 $m^2\ m^{-2}$, respectively, as these parameters had the largest effect on Penman-Monteith calculations. Fifteen iterations of dV_{WB} were used to quantify the uncertainty in dV_{WB} that results from the uncertainty in the input variables. The range of dV_{WB} is reported along with a dV_{WB} calculated with the preferred input values.

3.3.2. Baseflow Recession

Baseflow recession dynamics can provide insights into the consistency of baseflow sources. Baseflow recessions were calculated for 2009–2014 WYs during times when evapotranspiration, rainfall and snowmelt were negligible (Kirchner, 2009; Sayama et al., 2011). Nighttime data were used to reduce the influence of evapotranspiration. Late summer baseflow data (July and August) were used to eliminate the snowmelt pulse that dominated the hydrograph during spring and early summer. Days with more than 1 mm of rainfall 6 hr prior to nighttime were removed to eliminate the effects of rainfall. Recession slopes ($-\mathrm{d}Q/\mathrm{d}t$) and average discharge were calculated for 4-hr periods (Q_1: 19:00–22:59, Q_2: 23:00–2:59, Q_3: 3:00–6:59) to reduce small fluctuations in discharge that can be caused by instrument error (Sayama et al., 2011). For each period $-\mathrm{d}Q/\mathrm{d}t$ and Q were calculated as $(Q_1 - Q_2)/4$, $(Q_1 + Q_2)/2$, respectively, and $(Q_2 - Q_3)/4$, $(Q_2 + Q_3)/2$, respectively (Sayama et al., 2011).

Assuming discharge is a function of watershed storage, the recession slopes were used to estimate dV for each subwatershed as the difference in storage between average maximum and minimum discharge for the period outlined above (Buttle, 2016; Kirchner, 2009). To estimate the dynamic storage based on the baseflow recession (dV_{Bf}), the discharge sensitivity function, $g(Q)$, was calculated for the same times as above ($ET \approx 0$, $P = 0$; Kirchner, 2009):

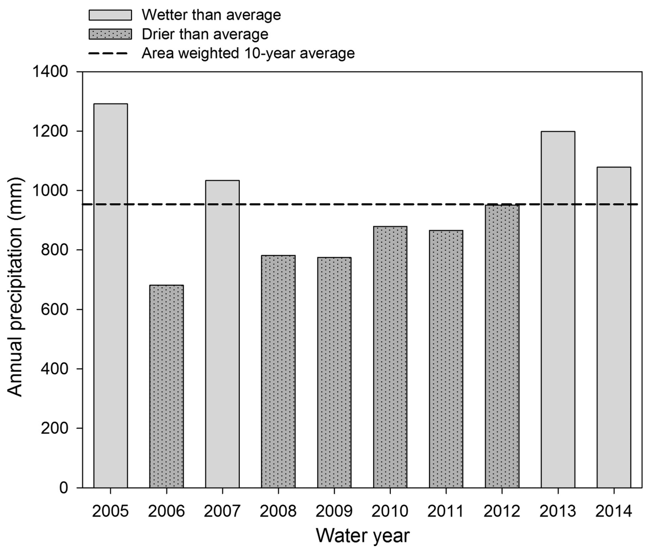

Figure 2. Area weighted annual precipitation for Star Creek watershed. The dashed line represents the 10-year mean annual precipitation across the water years of record.

$$g(Q) = \frac{dQ}{dS} \approx \frac{\frac{-dQ}{dt}}{Q} | P = 0, ET \approx 0 \tag{2}$$

This discharge sensitivity function can be rearranged to estimate dS as

$$\int dS = \int \frac{dQ}{g(Q)} \tag{3}$$

Mean Q and mean $-dQ/dt$ were calculated for binned ranges in Q that represented at least 1% of the range in Q and for which the standard error was smaller than half the mean flow (Kirchner, 2009). Binned means were transformed and plotted as $\ln(-dQ/dt)$ and $\ln(Q)$ and a quadratic equation was fit to the data. The quadratic equation was used to determine the coefficients for

$$\ln(g(Q)) = \ln\left(\frac{-dQ/dt}{Q}\right) \approx c_1 + c_2 \ln(Q) + c_3 (\ln(Q))^2 \tag{4}$$

Coefficients c_1 and c_3 come directly from the quadratic equation ($y = c_3 x^2 + kx + c_1$); c_2 was the recession slope (k) − 1 (Kirchner, 2009).

4. Results

4.1. Temporal Variation in Precipitation-Runoff Relationships

4.1.1. Multiyear Coupling

Comparison of the total annual precipitation for each WY to the 10-year average annual precipitation shows that there were clear wet and dry periods (Figure 2). Total precipitation between 2008 and 2011 WY was lower than the 10-year average annual precipitation (74–179 mm), while precipitation between 2013 and 2014 WY was higher than average (125–245 mm). Precipitation in 2012 was approximately average. The same analysis was performed for a longer-term precipitation record (1955–2016) from nearby Blairmore, AB (Alberta Climate Information Service; elevation of 1,310 m; ~10 km from Star Confluence) to determine if the dry and wet patterns associated with the 10-year record were visible in the longer 62-year record. The wet period had much greater precipitation than the 62-year average (235–291 mm), but the dry years were not consistent across the period. Precipitation during the 2007–2008 WYs was 16–96 mm below the long-term average, while precipitation during 2009–2011 was 77–274 mm greater. Despite this difference, we retained the classification of 2008–2011 as a dry period and 2013–2014 as a wet period from our 10-year data record because these data were based on a much denser network of precipitation gauges at various elevations throughout our specific study watersheds and it is not likely that storage patterns persist over multiple decades.

The transition from the multiyear dry period to multiyear wet period corresponded with an increase in annual streamflow (specific discharge) from 2009–2014 (Table 1). While considerable variation was observed between subwatersheds, most had lower than average specific discharge for 2009 and 2010 and above average specific discharge from 2012 to 2014. SWL changed from a losing subwatershed during the multiyear dry period to a strongly gaining subwatershed from 2012–2014. For SEL there was a weaker increase in specific discharge during the wet period. In general, the two alpine subwatersheds (SWU and SEU) contributed the largest portion of streamflow (as a percent) to the overall streamflow at the outlet at SM. The trend for Star Lower (SL), the subwatershed associated with the mainstem only (SL = SM-SE-SW-McLaren; Figure 1) was opposite from the other subwatersheds. In the dry period, there was greater specific discharge at the gauging site than total precipitation inputs to the watershed (mean $P = 840$ mm yr^{-1}; 2009–2011). In contrast, during the wet period SL showed a net loss of streamflow in 2014 with lower streamflow than the sum of upstream tributary inflows.

4.1.2. Short-Term Coupling

Despite the strong increase in specific discharge across multiyear dry to wet periods, there was no difference in the hydrograph response for event-based rainfall-runoff responses between the dry and wet period in SE

Table 1
Annual Specific Discharge Contribution (mm yr^{-1}) From Star West Upper (SWU), Star East Upper (SEU), Star West Lower (SWL), Star East Lower (SEL), and Star Lower (SL) Subwatersheds in Star Creek

Year	SWU	SEU	SWL	SEL	SL
2009	694	361	−48	119	934
2010	840	497	108	210	1,183
2011	1,228	633	−146	435	2,615
2012	1,025	743	356	405	600
2013	1,031	702	524	335	602
2014	900	706	994	593	−402
Mean	953	607	298	350	922
CV	0.19	0.25	1.42	0.48	1.07

or SW subwatersheds (Figure 3). There was also no obvious difference in runoff responses observed between summer months (July–September) despite differences in hillslope groundwater levels over these months (Figures 4a and 4b). Water levels in hillslope groundwater wells responded primarily to snowmelt pulses or large rainfall events during the spring at SEL, SM, and SWU; the SWL hillslope groundwater well remained dry year-round. For instance, the 50+ mm event in early June 2015 produced a response in all wells, whereas a similar event in early September 2015 only produced a small response in the SEL groundwater well (Figure 4b). Similar responses were also observed for hillslope wells in 2014 (Figure 4a).

The general relationship between winter precipitation and annual runoff ratios was poor. Rather, when antecedent conditions from the previous fall were accounted for, two trends in winter precipitation-runoff relations became evident (Figure 5). For years that were preceded by a wet fall, runoff ratios were higher than for years preceded by a dry fall.

4.2. Watershed Storage

4.2.1. Temporal Patterns

In contrast to the relationships between dV_{WB} and runoff that are typically observed in rainfall dominated systems, cumulative dV_{WB} and runoff relations produced counterclockwise patterns in these snow-dominated systems (Figure 6). The hysteresis observed here was due to the initial storage of snow above ground in winter months, followed by a sharp increase in discharge coincident with snowmelt, then a drainage period where both discharge and storage decreased. The overall range in cumulative dV_{WB} was smaller for 2006 and 2008–2011 (average: 217 and 263 mm for SW and SE, respectively) than for 2007 and 2012–2014 (average: 353 and 355 mm for SW and SE, respectively; Table 2). This pattern corresponded with the wet and dry precipitation periods (Figure 2) and the increased specific discharge (Table 1) because more water moved through the watershed in wet years than in dry years. An exception to this pattern was 2012, which was a transitional year with average precipitation but a large change in cumulative dV_{WB}.

4.2.2. Spatial Patterns

The differences in dV_{WB} between SE and SW subwatersheds were not consistent across years (Table 2); the ranges in dV_{WB} and the variation across years outweighed the variation between sites. However, the maximum dV_{WB} was larger in SW (462 mm) than SE (382 mm). Estimates of dV_{Bf} (from recession analysis) for July and August 2009–2014 showed a similar difference as the maximum dV_{WB}. SEL and SEU had the smallest dV_{Bf} (33 and 35 mm, respectively). SWL had the largest dV_{Bf} (118 mm) followed by SWU (52 mm).

Baseflow recession characteristics also differed between SE and SW. The minimum August specific discharge for SEL were lower than for SWL (Figure 7): In SWL it did not drop below 0.03 mm hr^{-1}, whereas in SEL streamflow dropped below 0.02 mm hr^{-1}. This suggests that baseflow in SWL had a more consistent source that maintained streamflow in late summer than in SEL. The small pond (0.25 ha) above SWL

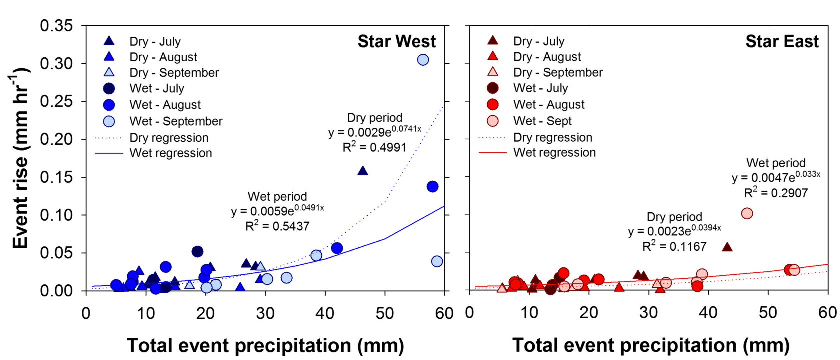

Figure 3. Event-based comparison between dry (triangles) and wet (circles) periods for SW and SE forks. Months are indicated by different ranges in color. Event rise (differences between specific discharge at the start of the event and peak specific discharge; mm hr^{-1}) as a function of event precipitation (mm).

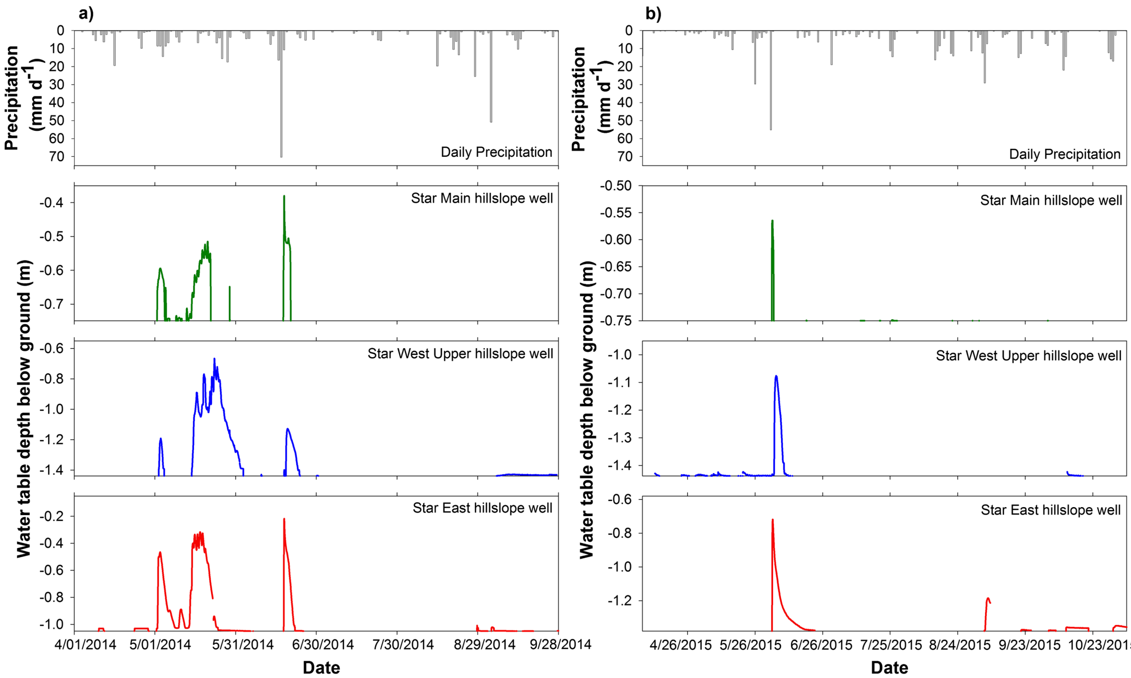

Figure 4. Hillslope well responses from three locations in Star Creek (Star Mainstem, SEL, SWU). (a) The 2014 water year. Hillslope responds during snowmelt and during large storm (70 mm) in early summer. Large storm (50 mm) in late summer only resulted in small groundwater well response. (b) The 2015 water year. Similar patterns were observed but drier conditions resulted in lower groundwater levels.

gauging station has an estimated volume of 5,000 m^3 and was likely not large enough to maintain late summer baseflow. The average discharge below the pond was 0.036 $m^3\ s^{-1}$ (3,110 $m^3\ day^{-1}$) in August 2015 which suggests that the pond would drain in 2 days if inputs stopped. Additionally, a similar pattern (higher specific discharge for SWL than SEL) was observed above the pond at SWU, in which baseflow in all years, except for 2012, did not fall below 0.04 mm hr^{-1} (Figure 7).

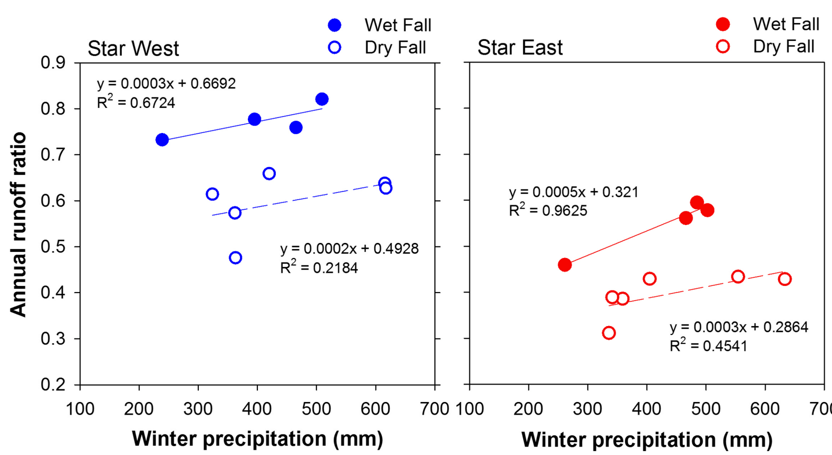

Figure 5. The relationship between annual runoff ratios and snowfall for SW (blue) and SE (red) watersheds. Closed circles represent years with wet conditions the previous fall. Open circles represent years with dry conditions the previous fall.

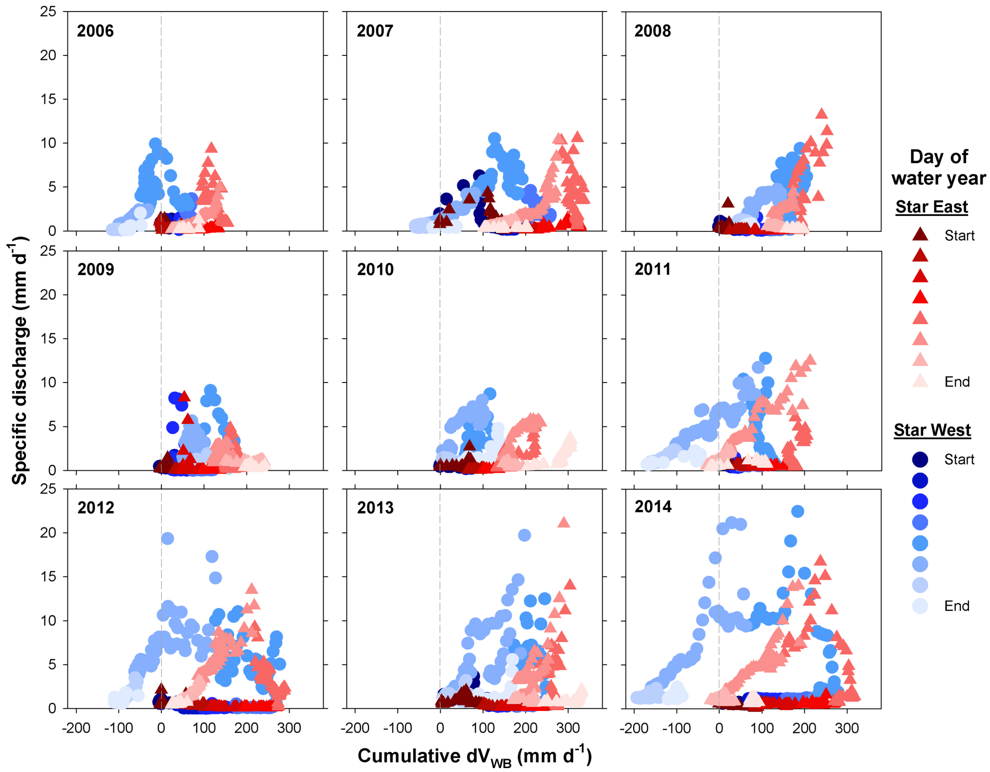

Figure 6. Relationship between watershed storage and stream discharge for 2006 to 2014 water years. SW in blue and SE in red. Water year starts at zero cumulative dV_{WB} (mm, gray dashed line) with darkest symbol color and transitions to lighter colors through the water year.

5. Discussion

5.1. Temporal Patterns in Precipitation-Runoff Relationships

We studied hydrological responses in Star Creek watershed during a dry period (2008–2011) and a wet period (2013–2014) (Figure 2). Sequential multiyear patterns of below or above average precipitation can draw down or fill watershed storage and influence streamflow responses (Devito et al., 2012). The influence of precipitation on streamflow was evident in annual specific discharge (Table 1). For most subwatersheds, specific discharge was lower than average specific discharge for WYs 2009–2010, whereas for WYs 2011–2014 specific discharge was above average. While this transition did not precisely match dry and wet years, the discharge pattern was consistent with the broader precipitation pattern. The patterns were consistent with the long-term 62-year precipitation pattern where much greater precipitation (270 mm) than average was observed from 2011–2014. Multiyear precipitation patterns have also been shown to influence watershed storage and runoff ratios in other regions (Nippgen et al., 2016; Tomasella et al., 2008). For instance, the precipitation from the previous year influenced runoff ratios the following year in Coweeta (Nippgen et al., 2016).

Although it appears that there were increases in precipitation and annual specific discharge over the years of record, this did not lead to differences in the precipitation-runoff relationships. Other studies showed that wet antecedent moisture conditions increase subsurface lateral flow and runoff to streams compared to dry antecedent conditions (Ali et al., 2015; Detty & McGuire, 2010a; Devito et al., 2012; Pfister et al., 2017) and we expected similar patterns for the multiyear wet and dry patterns. However, for neither SE nor SW watersheds was there a difference in runoff response between wet and dry years (Figure 3). The lack of difference may have been partly due to the strong control of snowmelt on groundwater storage. Shallow subsurface water tables (hillslope groundwater wells) responded primarily during snowmelt conditions (Figure 4). Smith et al. (2014) showed that snowmelt could overwhelm other runoff predictors (e.g., upslope contributing area and slope) during the spring freshet, which led to lateral flow in a snow-dominated watershed with deep glacial tills in southeast British Columbia. Similarly, Redding and Devito (2008)

10.1029/2019WR025313

Table 2
Range in Dynamic Storage (dV_{WB}; mm) for Water Years in Dry and Wet Periods and Dynamic Storage From Recession Analysis for July to August Baseflows (dV_{Bf}; mm)

	dV_{WB} (mm)			
	SW		SE	
Year	Range	dV_{WB}*	Range	dV_{WB}*
2006	127–231	178	142–219	174
2008	178–276	229	222–320	276
2009	151–290	208	198–354	280
2010	134–265	179	266–424	347
2011	231–341	289	238–301	238
Dry period mean		217		263
2007	288–358	303	285–450	373
2012	324–443	371	266–367	317
2013	224–358	277	282–499	382
2014	387–526	462	321–399	346
Wet period mean		353		355
dV_{Bf} (July/Aug)		SW		SE
Upper		52		35
Lower		118		33

Note. dV_{WB}* was calculated from the preferred values reported in section 3.3.1.

observed that while snowmelt in the Boreal forest can fill soil storage or overwhelm hydraulic conductivity mediated percolation and cause lateral flow, most rainfall events in that region do not. This suggests that although multiyear precipitation patterns regulated the baseflow component of the Star Creek hydrograph through vertical drainage in the soil or into the till, snowmelt and soil and glacial till storage were the primary controls on short-term runoff dynamics. This also suggests that this shallow subsurface zone functions as a different flow system than deeper bedrock storage. A similar two system storage was suggested for the Catskill Mountains in New York, another region with glacial till and permeable sedimentary bedrock (Burns et al., 1998).

Jenicek et al. (2016) and Nippgen et al. (2016) highlighted the importance of multitemporal scale precipitation patterns (monthly, seasonal, annual, and multiyear) in regulation of longer-term streamflow dynamics. Precipitation from September to mid-October (fall rainfall), during the period after evaporative losses from transpiration have declined or stopped, can fill soil and till storage and increase the subsequent year's runoff ratio. In cold regions, the extent of soil freezing can also be a major predictor of runoff and infiltration (Gray et al., 2001). More runoff can occur when infiltration is restricted due to the freezing of fully saturated soils. Conversely, unsaturated frozen soils lead to less runoff due to greater infiltration rates and more available storage capacity (Gray et al., 2001). In this study, the carryover of storage and differences in runoff were evident for both SE and SW subwatersheds (Figure 5). More specifically, years categorized as having a dry fall or wet fall did not correspond with

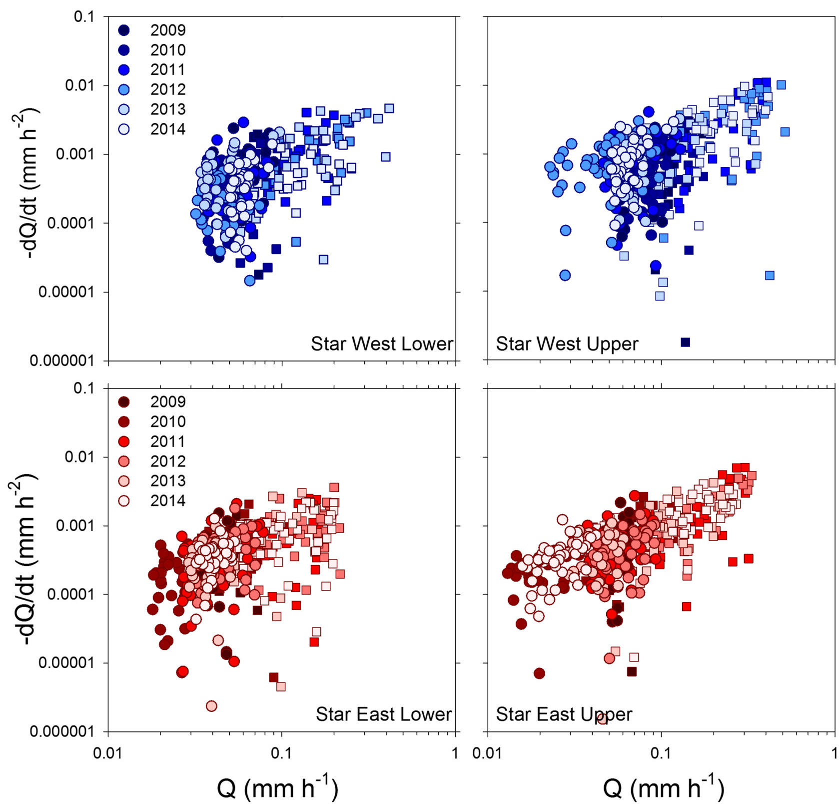

Figure 7. Recession analysis plots for Star West Lower (SWL), Star West Upper (SWU), Star East Lower (SEL), and Star East Upper (SEU). Squares represent July streamflow and circles represent August streamflow.

the multiyear dry and wet periods (Figure 2). These results are consistent with other studies showing that past precipitation can influence discharge on multiple temporal scales. For instance, groundwater fluctuations and streamflow had a multiyear memory reflecting precipitation from the previous years or seasons in a humid Amazonian watershed (Tomasella et al., 2008).

5.2. Spatial Patterns in Precipitation-Runoff Relationships

5.2.1. Subwatershed Comparison

Despite the lack of obvious differences in bedrock and surficial geology, there was considerable variation between subwatershed responses (Table 1). The pattern of transition from strongly increasing specific discharge (in excess of incoming precipitation) during dry years to average or decreasing specific discharge in wet years in the SL subwatershed was opposite to that in all other subwatersheds. The reason for this opposite trend is unclear. Watersheds with a history of glacial erosion and deposition can have complex subsurface flow pathways that are not visible in surface topography. For example, Langston et al. (2011) showed how a proglacial landscape (glacial alpine moraine) might contain features that are capable of blocking flow (e.g., ground ice and buried ice) and create complex connections and disconnections between surface water features. While Langston et al. (2011) examined water levels in lakes rather than streamflow, subsurface glacial features occur throughout a watershed and have the potential to interrupt or otherwise affect subsurface flow to streams as well. Similarly, Oda et al. (2013) showed that interwatershed transfer of groundwater in the Tanzawa Mountains, Japan, was responsible for greater streamflow in one watershed compared to the adjacent watershed, which had a net loss of groundwater. They related this to the effective drainage area, suggesting that the area contributing to streamflow was likely larger than the surface area due to differences in subsurface topography (Oda et al., 2013).

Variation in watershed structural components, such as slope, soil drainage, jointing, and faulting, can impose important additional hydrologic controls (Shanley et al., 2015). Structurally, the SW alpine region is surrounded by tall, near-vertical headwalls that represent a large subsurface hydraulic gradient and area for snow accumulation. In contrast, the SE alpine region has similar near vertical headwalls around part of the alpine region but is also partly surrounded by a more moderate, rounded peak and talus slopes of Mt. McLaren. Consequently, the SE alpine region does not have the same vertical hydraulic gradient that is present in SW and may not have the same folding or fracture patterns. Watershed elevation and, in turn, the increased influence of snow can directly affect streamflow such as summer low flows and drought sensitivity (Staudinger et al., 2015). Furthermore, the alpine area in SW contains water year-round in a marshy area due to the presence of cirque tills and the stream flows primarily over exposed bedrock below the outlet of the marshy area. Conversely, the stream channel in the SE alpine area is incised in colluvium with little exposed bedrock and goes dry midsummer. Other studies have shown that these kinds of structural components can lead to important differences in runoff generation processes (Gabrielli et al., 2012; Hale & McDonnell, 2016) and hydrograph recession even in topographically similar neighboring watersheds (Shanley et al., 2015).

5.2.2. Soil and Till Storage

While storage, represented by dV_{Bf} and dV_{WB} metrics, has been associated with streamflow response (Hale et al., 2016; McNamara et al., 2011; Sayama et al., 2011), dV_{WB} calculated using the water balance approaches has been almost exclusively examined for rainfall dominated watersheds (Hale et al., 2016; Pfister et al., 2017; Sayama et al., 2011). To our knowledge, Staudinger et al. (2017) was the first to use this analysis in snow dominated watersheds, but they did not describe the hysteretic pattern shown here. The timing of the subsurface disconnection of the hillslope and the stream (Figure 6) as dV_{WB} becomes negative (also reflected in the groundwater well responses) is an important metric associated with subsurface storage potential in the soil and glacial till. Thus, the range in cumulative dV_{WB} is important to compare different watersheds to assess potential differences in subsurface storage. The differences between SW and SE were not consistent across years nor were the ranges in dV_{WB} large enough to suggest one was larger than the other. However, dV_{Bf} estimates showed that SW had a larger storage than SE. These values were much smaller than dV_{WB} because they exclusively represent baseflow conditions when much less water moved through the system. Hillslope groundwater well responses further corroborate the difference between SE and SW watersheds because although all wells responded during snowmelt, only the SEL groundwater well responded in the late summer (Figure 4), again suggesting a smaller storage capacity than in SW. More wells are needed to substantiate these findings because hillslope groundwater levels can be influenced by many other factors, such as upslope accumulated area, variability in soils, and local slope (Detty & McGuire, 2010b; Jencso et al., 2009; Rinderer et al., 2014).

Maximum dV_{WB} estimates across all years (462 and 382 mm for SW and SE, respectively, Table 2) were slightly smaller than those reported by Hale et al. (2016) for a headwater watershed (485 mm) and at the downstream outlet (501 mm) in the Central Coast Range in Oregon, which has similar geology (highly fractured sedimentary bedrock) and shallow soils as Star Creek watershed but saprolite rather than glacial till. Hale et al. (2016) attributed their dV_{WB} values to subsurface storage in the saprolite and highly fractured upper layer of bedrock (2–10 m thick), noting that total storage was an order of magnitude higher when taking the deeper fractured bedrock into account. Sayama et al. (2011) also reported similar estimates (232–651 mm) in watersheds with highly weathered sedimentary bedrock in northern California. These large storage capacities reported here suggest that geologically similar watersheds should result in a large storage capacity. These watersheds may also have lower responsiveness to changes in precipitation forcing from forest disturbance or climate change than may be expected for other mountainous regions with shallower soils or tills and less permeable bedrock.

5.2.3. Bedrock Storage

Bedrock storage cannot be estimated without the use of hydrological models (Kosugi et al., 2011; Shaw et al., 2013; Staudinger et al., 2017) or isotopes (Ajami et al., 2011; Hale et al., 2016). However, recession analysis can provide insights into the consistency of baseflow or groundwater sources to estimate differences in bedrock storage (Sayama et al., 2011). August baseflows (specific discharge) in SEU were lower than in SWU (Figure 7) suggesting SWU had more consistent groundwater sources that maintained baseflow above 0.04 mm hr^{-1}, whereas the source of baseflow in SEU became depleted through the summer. This suggests that SW has a greater bedrock storage capacity than SE. This was also reflected in the temporal variability (coefficient of variation) of subwatershed specific discharge (Table 1), which was less variable between years for SWU than SEU (CV = 0.19 and 0.25, respectively; Figure S2 in the supporting information). Other studies have shown that larger bedrock storage can result in higher or more stable baseflow (Burns et al., 1998; Pfister et al., 2017; Shanley et al., 2015; Staudinger et al., 2015; Uchida et al., 2006). While Shanley et al. (2015) showed that high storage capacity and low permeability dense glacial till in Vermont, USA, could sustain baseflow through the slow release of groundwater, the persistence of snow and a larger storage capacity were responsible for maintaining flows during drought years in high elevation watersheds in Switzerland compared to lower elevation watersheds (Staudinger et al., 2015).

Many other studies stress geologic and subsurface characteristics (e.g., fractures and porosity) as key factors that determine the storage capacity (Gabrielli et al., 2012; Pfister et al., 2017; Uchida et al., 2006). Gabrielli et al. (2012) hypothesized that fractured bedrock added an additional flow pathway and resulted in seepage losses in the HJ Andrews watershed in western United States, compared to the relatively impermeable Maimai watershed in New Zealand. Uchida et al. (2006) compared two relatively similar watersheds, Fudoji watershed in Japan (permeable bedrock) to Maimai watershed in New Zealand (less permeable bedrock) and showed that more permeable bedrock resulted in a greater storage capacity. In general, we hypothesize that the fractured bedrock and the permeable glacial till in Star Creek resulted in large storage and promoted deep percolation rather than lateral flow for much of the year (Figure 4). While there were no notable differences in subsurface characteristics observed during well installations, nor evident in bedrock outcrops, extensive subsurface characterization was not possible across the 10 km^2 watershed. Thus, it is unclear whether differences in bedrock permeability due to fracturing or glacial till depth or texture were the key factors driving the differences in runoff dynamics we observed between the SE and SW subwatersheds.

5.3. Runoff Mechanisms and the Implications for Hydrologic Change

The results of this study provide important conceptual insights into higher-order controls on precipitation-runoff dynamics exerted by watershed storage in postglacial mountain regions with permeable fractured bedrock. The precipitation-runoff and storage dynamics observed here were used to develop a conceptual understanding of runoff generation in this region. While recent studies have shown that fractured or permeable bedrock was a key subsurface storage zone (Chen et al., 2018; Hale & McDonnell, 2016; Uchida et al., 2006) and deep soils or glacial till create complex subsurface flow pathways and large subsurface storage (Dahlke et al., 2012; Kuras et al., 2008; Shanley et al., 2015), no other study has thus far quantified storage

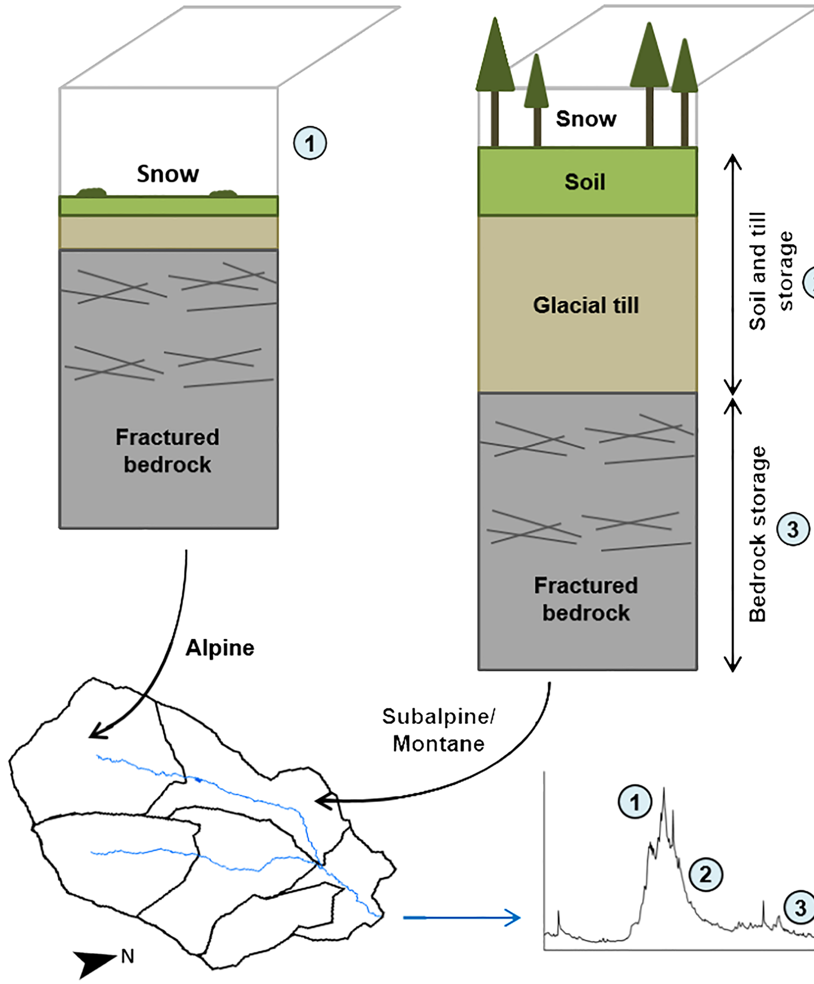

Figure 8. Conceptual block diagram of storage zones for alpine and subalpine regions in Star Creek watershed and the eastern slopes of the Rocky Mountains. Hydrograph was compiled from mean daily discharge at SM station at the outlet of Star Creek watershed. Numbers on block diagrams and hydrograph refer to the portion of the landscape that is driving the corresponding portion of the hydrograph.

in a region with both unconsolidated glacial till and permeable bedrock. The combination of glacial till and permeable fractured bedrock adds complexity to runoff generation dynamics (Burns et al., 1998) that likely lead to the lack of hydrologic change following forest disturbance observed in the eastern slopes of the Canadian Rocky Mountains (Goodbrand & Anderson, 2016; Harder et al., 2015; Williams et al., 2015). The results described here suggest there were likely two zones of storage within these watersheds: soil and till storage ((2) in Figure 8) and bedrock storage (fractured bedrock; (3) in Figure 8). Soil and till storage was likely important for the carryover of precipitation and streamflow responses during snowmelt or for large events in late summer. Hillslope groundwater wells responded only during snowmelt and during larger events (Figure 4) likely due to a large soil and till storage capacity. Event-based analyses showed no difference between multiyear wet and dry periods (Figure 3) because event flows were mediated by snowmelt ((1) in Figure 8) and soil and till storage rather than bedrock storage. Isotopic analyses are needed to determine the approximate age of the stored water and confirm these interpretations. Further separation of storage in soil and glacial till requires analysis of water chemistry data and installation of wells in the till to determine how responses between these layers differ. Quantifying soil characteristics, such as porosity, water retention, and saturated hydraulic conductivity, would further clarify the differences between these layers.

Annual discharge patterns were affected by multiyear precipitation patterns, which were likely more strongly influenced by bedrock storage (Table 1). The influence of variation in multiyear precipitation may have only been observable from spatial patterns in subwatershed annual specific discharge and not the event-scale runoff because at the annual time step baseflow was a major contributor to streamflow (~70% of annual flow; Wagner et al., 2014—estimated using the recursive digital filter method by Nathan and McMahon (1990)).

Watersheds with steep slopes, permeable bedrock, and deep soils or glacial till have potentially a large storage capacity and, in turn, may retain excess water and buffer the stream from change (Harder et al., 2015). Conversely, watersheds with steep slopes and shallow bedrock may be more responsive to disturbance because there is little storage for the excess water to be retained. These results aid in the interpretation of streamflow responses following disturbance in watershed scale studies. Rather than focusing on the specific differences in runoff generation processes for watersheds, we can focus on larger storage features (Buttle, 2016; McNamara et al., 2011) and watershed responsiveness (Carey et al., 2010) to determine whether a streamflow may or may not change following disturbance.

6. Conclusions

The study period changed from dry (2008–2011) to wet (2013–2014), which caused an increase in specific discharge for all but one subwatershed. Despite a corresponding change in annual flow, event-scale rainfall-runoff responses did not change. Annual runoff ratios were influenced by the carryover of storage from the previous fall and were larger following a wetter fall than a drier fall. Two zones of subsurface storage were identified based on precipitation-runoff dynamics and storage estimates: soil and till storage and bedrock storage. Soil and till storage influences event runoff, hillslope connectedness controlled by snowmelt, and the carryover of precipitation from fall to the next water year. Bedrock storage influences annual discharge because of the dominance of vertical infiltration and groundwater recharge and high groundwater contribution to annual streamflow. Understanding these runoff generation mechanisms and the variation in precipitation-runoff response is important for understanding how a watershed might respond to disturbance or climate change.

Acknowledgments
The authors would like to acknowledge funding support from Alberta Agriculture and Forestry, Alberta Innovates Water Innovation Program, Forest Resource Improvement Association of Alberta (FRIAA), Canfor, and the Natural Sciences and Engineering Research Council (NSERC) of Canada. This work would not have been possible without the help of Jessica Snedden, Jamie Farkvam, Jocelyn Howery, Jeremy Fitzpatrick, Sarah Euler, Eddie Noton, Jolene Lust, Ian Tichkowsky, Lance Steinke, Jem Morrison, Samantha Karpyshin, Amanda Martens, Ashley Peter-Rennich, Lori Thorsen, Melaina Weiss, Evan Esch, Veronica Martens, Eric Lastiwka, Kirk Hawthorn, Kalli Herlein, Mike Wagner, and Chris Williams for field work and data QA/QC. We would like to thank Kevin Devito for his contribution to ideas during the initial stages of this research and Jim Buttle for assistance with the dynamic storage analysis. We would also like to thank Sean Carey and two anonymous reviewers for their thoughtful comments and for significant improvements to this manuscript. The authors declare no conflicts of interest. Supporting data are available in tables within the manuscript or online (https://doi.org/10.7939/DVN/IJBJRE). Funding Information: ESRD 69GRFD17; AIEES 2343, AIBio 16-009; Canfor/FRIAA FFI-15-010; and NSERC Discovery Grant 2006-05497.

References

AGS, Alberta Geological Survey (2004). Bedrock geology of Alberta (GIS data). Accessed from: www.ags.gov.ab.ca.

Ajami, H., Troch, P. A., Maddock, T., Meixner, T., & Eastoe, C. (2011). Quantifying mountain block recharge by means of catchment-scale storage-discharge relationships. *Water Resources Research*, *47*, W04504. http://doi.org/10.1029/2010ER009598

Ali, G., Tetzlaff, D., McDonnell, J. J., Soulsby, C., Carey, S., Laudon, H., et al. (2015). Comparison of threshold hydrologic response across northern catchments. *Hydrological Processes*, *29*(16), 3575–3591. https://doi.org/10.1002/hyp.10527

AVI, Alberta Vegetation Inventory (2010). Alberta vegetation inventory (AVI) crown (GIS data). Forest Management Branch, Forestry Division, Alberta Agriculture and Forestry. Government of Alberta.

Boon, S. (2012). Snow accumulation following forest disturbance. *Ecohydrology*, *5*(3), 279–285. https://doi.org/10.1002/eco.212

Brabender, B. (2005). Scaling leaf area index and rainfall interception in lodgepole pine. MSc. thesis. University of Alberta, Edmonton, AB.

Burns, D. A., Murdoch, P. S., Lawrence, G. B., & Michel, R. L. (1998). Effect of groundwater springs on NO_3^- concentrations during summer in Catskill Mountain streams. *Water Resources Research*, *34*(8), 1987–1996.

Buttle, J. M. (2016). Dynamic storage: A potential metric of inter-basin differences in storage properties. *Hydrological Processes*, *30*, 4644–4653. https://doi.org/10.1002/hyp.10931

Buttle, J. M., Dillon, P. J., & Eerkes, G. R. (2004). Hydrologic coupling of slopes, riparian zones and streams: An example from the Canadian Shield. *Journal of Hydrology*, *287*, 161–177.

Carey, S. K., Tetzlaff, D., Seibert, J., Soulsby, C., Buttle, J., Laudon, H., et al. (2010). Inter-comparison of hydro-climatic regimes across northern catchments: Synchronicity, resistance and resilience. *Hydrological Processes*, *24*(24), 3591–3602. https://doi.org/10.1002/hyp.7880

Carlson, T. N. (1991). Modeling stomatal resistance: an overview of the 1989 workshop at the Pennsylvania State University. *Agricultural and Forest Meteorology*, *54*, 103–106.

Chen, Z., Hartmann, A., Wagener, T., & Goldscheider, N. (2018). Dynamics of water fluxes and storages in an Alpine karst catchment under current and potential future climate conditions. *Hydrology and Earth System Sciences*, *22*(7), 3807–3823. http://doi.org/10.5194/hess-22-3807-2018

Cherlet, E., Williams, C. H. S., Herlein, K., Hawthorn, K., & Silins, U. (2018). Evaluating accuracy of simple winter precipitation overspill systems with tipping bucket gauges for winter precipitation monitoring in remote mountain weather station networks. American Geophysical Union, Fall Meeting 2018, Abstract ID: H13P-1980, Washington, D.C., USA.

Dahlke, H. E., Easton, Z. M., Lyon, S. W., Walter, M. T., Destouni, G., & Steenhuis, T. S. (2012). Dissecting the variable source area concept-subsurface flow pathways and water mixing processes in a hillslope. *Journal of Hydrology*, *420*, 125–141. http://doi.org/10.1016/j.hydrol.2011.11.052

Detty, J. M., & McGuire, K. J. (2010a). Threshold changes in storm runoff generation at a till mantled headwater catchment. *Water Resources Research*, *46*, W07525. http://doi.org/10.1029/2009WR008102

Detty, J. M., & McGuire, K. J. (2010b). Topographic controls on shallow groundwater dynamics: implications for hydrologic connectivity between hillslopes and riparian zones in a till mantled catchment. *Hydrological Processes*, *24*(16), 2222–2236. http://doi.org/10.1002/hyp.7656

Devito, K., Mendoza, C., & Qualizza, C. (2012). Conceptualizing water movement in the Boreal Plains. Implications for watershed reconstruction. Synthesis report prepared for the Canadian Oil Sands Network for Research and Development, Environmental and Reclamation Research Group. 164 pp.

Dixon, D., Boon, S., & Silins, U. (2014). Watershed-scale controls on snow accumulation in a small montane watershed, southwestern Alberta, Canada. *Hydrological Processes*, *28*, 1294–1306. https://doi.org/10.1002/hyp.9667

Gabrielli, C. P., McDonnell, J. J., & Jarvis, W. T. (2012). The role of bedrock groundwater in rainfall-runoff response at hillslope and catchment scales. *Journal of Hydrology*, *450*, 117–133. https://doi.org/10.1016/j.jhydrol.2012.05.023

Gannon, J. P., Bailey, S. W., & McGuire, K. J. (2014). Organizing groundwater regimes and response thresholds by soils: A framework for understanding runoff generation in a headwater catchment. *Water Resources Research*, *50*, 8403–8419. http://doi.org/10.1002/2014WR015498

Goodbrand, A. & Anderson, A. (2016). Hydrologic resilience of a Canadian Foothills watershed to forest harvest. Geophysical Research Abstracts, 18, EGU2016-10932. EGU General Assembly 2016, Vienna, Austria.

Government AB (2000). State of the Environment Report. Chapter 2: Origin and distribution of surface water in Alberta.

Gray, D. M., Toth, B., Zhao, L., Pomeroy, J. W., & Granger, R. J. (2001). Estimating areal snowmelt infiltration into frozen soils. *Hydrological Processes*, *15*(16), 3095–3111. http://doi.org/10.1002/hyp.320

Hale, V. C., & McDonnell, J. J. (2016). Effect of bedrock permeability on stream base flow mean transit time scaling relations: 1. A multiscale catchment intercomparison. *Water Resources Research*, *52*, 1358–1374. https://doi.org/10.1002/2014WR016124

Hale, V. C., McDonnell, J. J., Stewart, M. K., Solomon, D. K., Doolitte, J., Ice, G. G., & Pack, R. T. (2016). Effect of bedrock permeability on stream base flow mean transit time scaling relationships: 2. Process study of storage and release. *Water Resources Research*, *52*, 1375–1397. https://doi.org/10.1002/2015WR017660

Harder, P., Pomeroy, J. W., & Westbrook, C. J. (2015). Hydrological resilience of a Canadian Rockies headwaters basin subject to changing climate, extreme weather, and forest management. *Hydrological Processes*, *29*, 3905–3924. https://doi.org/10.1002/hyp.10596

Hewlett, J. D., & Hibbert, A. R. (1967). Factors affecting the response of small watersheds to precipitation in humid areas. *Forest Hydrology*, *1*, 275–290.

Hood, J. L., & Hayashi, M. (2015). Characterization of snowmelt flux and groundwater storage in an alpine headwater basin. *Journal of Hydrology*, *521*, 482–497. https://doi.org/10.1016/j.hydrol.2014.12.041

Jencso, K. G., McGlynn, B. L., Gooseff, M. N., Wondzell, S. M., Bencala, K. E., & Marshall, L. A. (2009). Hydrologic connectivity between landscapes and streams: Transferring reach-and plot-scale understanding to the catchment scale. *Water Resources Research*, *45*, W04428. https://doi.org/10.1029/2008WR007225

Jenicek, M., Seibert, J., Zappa, M., Staudinger, M., & Jonas, T. (2016). Importance of maximum snow accumulation for summer low flows in humid catchments. *Hydrology and Earth System Sciences*, *20*, 859–874. https://doi.org/10.5194/hess-20-859-2016

Karpyshin, S. (2019). Transpiration response of residual lodgepole pine after partial-cut and strip-shelterwood harvesting in Alberta's southern Rocky Mountains. MSc. thesis. University of Alberta, Edmonton, AB.

Kienzle, S. W. (2008). A new temperature based method to separate rain and snow. *Hydrological Processes*, *22*, 5067–5085. http://doi.org/10.1002/hyp.7131

Kirchner, J. W. (2009). Catchments as simple dynamical systems: Catchment characterization, rainfall-runoff modeling, and doing hydrology backward. *Water Resources Research*, *45*, W02429. https://doi.org/10.1029/2008WR006912

Kosugi, K. I., Fujimoto, M., Katsura, S. Y., Kato, H., Sando, Y., & Mizuyama, T. (2011). Localized bedrock aquifer distribution explains discharge from a headwater catchment. *Water Resources Research*, *47*, W07530. http://doi.org/10.1029/2010WR009884

Kuras, P. K., Weiler, M., & Alila, Y. (2008). The spatiotemporal variability of runoff generation and groundwater dynamics in a snow-dominated catchment. *Journal of Hydrology*, *352*, 50–66. https://doi.org/10.1016/j.jhydrol.2007.12.021

Langston, G., Bentley, L. R., Hayashi, M., McClymont, A., & Pidlisecky, A. (2011). Internal structure and hydrological functions of an alpine proglacial moraine. *Hydrological Processes*, *25*, 2967–2982. https://doi.org/10.1002/hyp.8144

MacDonald, M. K., Pomeroy, J. W., & Pietroniro, A. (2010). On the importance of sublimation to an alpine snow mass balance in the Canadian Rocky Mountains. *Hydrology and Earth System Sciences*, *14*, 1401–1415. https://doi.org/10.5194/hess-14-1401-2010

McClymont, A. F., Hayashi, M., Bentley, L. R., Muir, D., & Ernst, E. (2010). Groundwater flow and storage within an alpine meadow-talus complex. *Hydrology and Earth System Sciences*, *14*(6), 859–872. http://doi.org/10.5194/hess-14-859-2010

McGuire, K. J., McDonnell, J. J., Weiler, M., Kendall, C., McGlynn, B. L., Welker, J. M., & Seibert, J. (2005). The role of topography on catchment-scale water residence time. *Water Resources Research*, *41*, W05002. https://doi.org/10.1029/2004WR003657

McNamara, J. P., Tetzlaff, D., Bishop, K., Soulsby, C., Seyfried, M., Peters, N. E., et al. (2011). Storage as a metric of catchment comparison. *Hydrological Processes*, *25*(21), 3364–3371. https://doi.org/10.1002/hyp.8113

Monteith, J. L. (1965). Evaporation and environment. *Symposia of the Society for Experimental Biology*, *19*, 205–234.

Mosley, M. P. (1979). Streamflow generation in a forested watershed, New Zealand. *Water Resources Research*, *15*, 795–806. https://doi.org/10.1029/WR015i004p00795

Nathan, R. J., & McMahon, T. A. (1990). Evaluation of automated techniques for base flow and recession analyses. *Water Resources Research*, *26*(7), 1465–1473.

Nippgen, F., McGlynn, B. L., Emanuel, R. E., & Vose, J. M. (2016). Watershed memory at the Coweeta Hydrologic Laboratory: The effect of past precipitation and storage on hydrologic response. *Water Resources Research*, *52*, 1673–1695. https://doi.org/10.1002/2015WR018196

Oda, T., Masakazu, S., Egusa, T., & Uchiyama, Y. (2013). Effect of bedrock flow on catchment rainfall-runoff characteristics and the water balance in forested catchments in Tanzawa Mountains, Japan. *Hydrological Processes*, *27*, 3864–3872. https://doi.org/10.1002/hyp.9497

Pfister, L., Martínez-Carreras, N., Hissler, C., Klaus, J., Carrer, G. E., Stewart, M. K., & McDonnell, J. J. (2017). Bedrock geology controls on catchment storage, mixing, and release: A comparative analysis of 16 nested catchments. *Hydrological Processes*, *31*, 1828–1845. https://doi.org/10.1002/hyp.11134

Pomeroy, J. W. & Schmidt, R. A. (1993). The use of fractal geometry in modelling intercepted snow accumulation and sublimation. Proceedings of the 50th Eastern Snow Conference, Quebec City, QC, Eastern Snow Conference, 1-10.

Rasouli, K., Pomeroy, J. W., & Whitfield, P. H. (2019). Hydrological responses of headwater basins to monthly perturbed climate in the North American cordillera. *Journal of Hydrometeorology*. http://doi.org/10.1175/JHM-D-18-0166.1

Redding, T., & Devito, K. (2008). Lateral flow thresholds for aspen forested hillslopes on the Western Boreal Plain, Alberta, Canada. *Hydrological Processes*, *22*, 4287–4300. https://doi.org/10.1002/hyp.7038

Rinderer, M., van Meerveld, H. J., & Seibert, J. (2014). Topographic controls on shallow groundwater levels in a steep, prealpine catchment: When are the TWI assumptions valid? *Water Resources Research*, *50*, 6067–6080. http://doi.org/10.1002/2013WR015009
Sayama, T., McDonnell, J. J., Dhakal, A., & Sullivan, K. (2011). How much water can a watershed store? *Hydrological Processes*, *25*, 3899–3908. https://doi.org/10.1002/hyp.8288
Shaman, J., Stieglitz, M., & Burns, D. (2004). Are big basins just the sum of small catchments? *Hydrological Processes*, *18*(16), 3195–3206.
Shanley, J. B., Sebestyen, S. D., McDonnell, J. J., McGlynn, B. L., & Dunne, T. (2015). Water's Way at Sleepers River watershed–revisiting flow generation in a post-glacial landscape, Vermont USA. *Hydrological Processes*, *29*, 3447–3459. https://doi.org/10.1002/hyp.10377
Shaw, S. B., McHardy, T. M., & Riha, S. J. (2013). Evaluating the influence of watershed moisture storage on variations in base flow recession rates during prolonged rain-free periods in medium-sized catchments in New York and Illinois, USA. *Water Resources Research*, *49*, 6022–6028. http://doi.org/10.1002/wrcr.20507
Silins, U., Stone, M., Emelko, M. B., & Bladon, K. D. (2009). Sediment production following severe wildfire and post-fire salvage logging in the Rocky Mountain headwaters of the Oldman River Basin, Alberta. *Catena*, *79*, 189–197. https://doi.org/10.1016/j.catena.2009.04.001
Smith, R., Moore, R., Weiler, M., & Jost, G. (2014). Spatial controls on groundwater response dynamics in a snowmelt-dominated montane catchment. *Hydrology and Earth System Sciences*, *18*, 1835–1856. https://doi.org/10.5194/hess-18-1835-2014
Smith, R., & Redding, T. (2012). Cumulative effects assessment: Runoff generation in snowmelt dominated montane and boreal plain catchments. *Streamline Watershed Management Bulletin*, *15*, 24–34.
Staudinger, M., Stoelzle, M., Seeger, S., Seibert, J., Weiler, M., & Stahl, K. (2017). Catchment water storage variation with elevation. *Hydrological Processes*, *31*, 2000–2015. https://doi.org/10.1002/hyp.11158
Staudinger, M., Weiler, M., & Seibert, J. (2015). Quantifying sensitivity to droughts—An experimental modeling approach. *Hydrology and Earth System Sciences*, *19*, 1371–1384. https://doi.org/10.5194/hess-19-1371-2015
Stednick, J. D. (1996). Monitoring the effects of timber harvest on annual water yield. *Journal of Hydrology*, *176*(1-4), 79–95. https://doi.org/10.1016/0022-1694(95)02780-7
Stewart, J. B. (1988). Modelling surface conductance of pine forest. *Agriculture and Forest Meteorology*, *43*, 19–35.
Tomasella, J., Hodnett, M. G., Cuartas, L. A., Nobre, A. D., Waterloo, M. J., & Oliveira, S. M. (2008). The water balance of an Amazonian micro-catchment: The effect of interannual variability of rainfall on hydrological behaviour. *Hydrological Processes*, *22*, 2133–2147. https://doi.org/10.1002/hyp.6813
Troendle, C. A. & Meiman, J. R. (1986). The effect of patch clear-cutting on the water balance of a subalpine forest slope. Proceedings of the 54th Western Snow Conference, Phoenix, AZ, Western Snow Conference, 93-100.
Uchida, T., Asano, Y., Ohte, N., & Mizuyama, T. (2003). Analysis of flowpath dynamics in a steep unchannelled hollow in the Tanakami Mountains of Japan. *Hydrological Processes*, *17*, 417–430. https://doi.org/10.1002/hyp.1133
Uchida, T., McDonnell, J. J., & Asano, Y. (2006). Functional intercomparison of hillslopes and small catchments by examining water source, flowpath and mean residence time. *Journal of Hydrology*, *327*, 627–642. https://doi.org/10.1016/j.jhydrol.2006.02.037
Wagner, M. J., Bladon, K. D., Silins, U., Williams, C. H. S., Martens, A. M., Boon, S., et al. (2014). Catchment-scale stream temperature response to land disturbance by wildfire governed by surface-subsurface energy exchange and atmospheric controls. *Journal of Hydrology*, *517*, 328–338. https://doi.org/10.1016/j.jhydrol.2014.05.006
Williams, C., Silins, U., Bladon, K. D., Martens, A. M., Wagner, M. J., & Anderson, A. (2015). Rainfall-runoff dynamics following wildfire in mountainous headwater catchments, Alberta, Canada. American Geophysical Union, Fall Meeting 2015, Abstract ID: H34B-06, San Francisco, USA.
Williams, C. H. S., Silins, U., Spencer, S. A., Wagner, M. J., Stone, M., & Emelko, M. B. (2019). Net precipitation in burned and unburned subalpine forest stands after wildfire in the northern Rocky Mountains. *International Journal of Wildland Fire*. http://doi.org/10.1071/WF18181
Winkler, R., Spittlehouse, D., & Boon, S. (2017). Streamflow response to clear-cut logging on British Columbia's Okanagan Plateau. *Ecohydrology*, *10*(2), e1836. http://doi.org/10.1002/eco.1836